ORIGINAL ARTICLE

Rapid detection of Cr(VI) by AgNPs probe produced by *Anacardium occidentale* fresh leaf extracts

C. K. Balavigneswaran · T. Sujin Jeba Kumar ·
R. Moses Packiaraj · S. Prakash

Abstract Nowadays necessities for the green synthesis of nanoparticles are enlarged because of its neutral toxicity and eco-friendly advantages. In this present study, we have explored the rapid biosynthesis of AgNPs at room temperature by the fresh leaf aqueous extract of *Anacardium occidentale*. Aqueous extracts were prepared at different temperatures 60, 80 and 100 °C. Formation of silver nanoparticles (AgNPs) was confirmed by surface plasmon resonance (SPR) peak observed around 400–420 nm in UV–Visible spectra. Among the extracts prepared, 80 °C extract showed good shift in UV–Visible spectrum during Cr(VI) detection and a good linear relationship was found between the absorbance ratio (A_{510}/A_{400}) against 100 mM–1 µM concentration of Cr(VI). Cr(VI) was confirmed by the red shift of SPR position from 400 to 510 nm. Detection limit of our prepared probe is 1 µM and this simple technique exhibiting high selectivity to Cr(VI) over other tested heavy metal ions. Finally, efficient 80 °C extract synthesized AgNPs were characterized by XRD, SEM and TEM. XRD characterization confirmed its face centered cubic structure and confirmed that the prepared AgNPs are crystalline in nature. TEM and SEM characterization results revealed that the AgNPs are in spherical nature. The size of AgNPs was found to be 40–60 nm.

Introduction

Nanoparticles/nanomaterials are of great interest in the scientific community because of their unique properties and they bridge the gap between bulk materials and atomic or molecular structures. A bulk material has constant physical properties regardless of its size, but at the nanoscale this is often not the case. One of the examples are nanoparticles possess a very high aspect ratio.

Noble metal nanoparticles are intensely studied due to their unique optical, electrical and catalytic properties and it is being used in the fields of medicine, biology, material science, physics and chemistry. To utilize and optimize chemical or physical properties of nano-sized metal particles, a large spectrum of research has been focused to control the size and shape, which is crucial in tuning their physical, chemical and optical properties (Alivisatos 1996; Coe et al. 2002; Moronne et al. 1998). Various techniques, including chemical and physical methods have been developed to prepare metal nanoparticles, such as chemical reduction (Yu 2007; Tan et al. 2002; Petit et al. 1993; Vorobyova et al. 1999), electrochemical reduction (Liu and Lin 2004; Sandmann et al. 2000), photochemical reduction (Mallick et al. 2005; Keki et al. 2000), heat evaporation (Bae et al. 2002; Smetana et al. 2005), Langmuir–Blodgett (Zhang et al. 2006; Swami et al. 2004) and biological techniques (Naik et al. 2002) and so on. In most cases, the surface passivator reagents are needed to prevent

C. K. Balavigneswaran (✉) · T. Sujin Jeba Kumar ·
R. Moses Packiaraj · S. Prakash (✉)
Department of Biotechnology, Udaya School of Engineering
(Anna University Affiliated R & D Centre), Udaya Nagar,
Vellamodi, Kanyakumari District 628202, Tamil Nadu, India
e-mail: balaa02@gmail.com

S. Prakash
e-mail: pra_cas@yahoo.co.in

nanoparticles from aggregation. Unfortunately, many organic passivators are toxic and enough to pollute the environment if large scale nanoparticles are produced.

Biosynthesis of nanoparticles has received considerable attention in material synthesis field due to the growing need to develop environmentally benign technologies and to reduce the use or generation of hazardous substances to human health and the environment. This approach provides a facile and convenient entry for producing multiple inorganic NPs, especially metal nanoparticles, such as Ag, Au, Pt and Pd have been synthesized by different methods, including bacteria (Husseiny et al. 2007), fungi (Sastry et al. 2003) and plants (Sharma et al. 2007). Microbe-mediated synthesis of nanoparticles is not industrially feasible as they require the maintenance of highly aseptic conditions (Sathishkumar et al. 2009).

The use of plant extract for the synthesis of nanoparticles is a relatively under exploited field and is recently gaining wide attention and could be advantageous over other environmentally benign biological processes by eliminating the elaborate process of maintaining cell cultures. Plants that secrete the functional molecules for the reaction is compatible with the green chemistry principles. Advantages of using this biomaterial are (1) ecofriendly, (2) the reducing agents employed, and (3) the capping agent in the reaction. Jose-Yacaman and co-workers (Gardea-Torresdey et al. 2002, 2003) first reported the formation gold and silver nanoparticles by living plants. Green silver nanoparticles have been synthesized using various natural products, such as green tea (*Camellia sinensis*) (Vilchis-Nestor et al. 2008), neem (*Azadirachta indica*) leaf broth (Shiv Shankar et al. 2004), natural rubber (Abu Bakar et al. 2007), starch (Vigneshwaran et al. 2006), aloevera plant extract (Chandran et al. 2006), lemongrass leaves extract (Shankar et al. 2004, 2005) leguminous shrub (*Sesbania drummondii*) (Sharma et al. 2007), mushroom extract (Philip 2009), Coleus amboinicus lour (Narayanan and Sakthivel 2011), *Medicago sativa* (Lukman et al. 2011), and *Citrus sinensis* peel (Kaviya et al. 2011) to name few.

Shankar et al. (2004) and Shiv Shankar et al. (2004) reported the metallic silver and gold nanoparticle synthesis by using Neem (*Azadirachta indica*) leaf broth. The time required for >90 % reduction of Ag^+ and Au^{3+} ions using Neem leaf broth was approximately 4 and 2 h, respectively. To enable the biological methods of nanoparticle synthesis to compete with the chemical methods, there is a need to achieve faster synthesis rates with good stability.

In the last few decades, there has been a considerable increase in release of chromium in aquatic and terrestrial ecosystems as a consequence of anthropogenic activities (Basu et al. 2010; Broadhurst and Domenico 2006). Oxidation state of chromium determines its level of toxicity.

Hexavalent chromium [Cr(VI)] is highly soluble, thus it is biologically available in the ecosystems. Cr(III) is an essential nutrient for maintaining normal physiological function (Wang et al. 2004), whereas Cr(VI) is about 100–1,000 times more toxic than the trivalent form (Sarkar et al. 2006). It is considered as a severe environmental pollutant, due to its highly carcinogenic properties (Zhang et al. 2009; Wu et al. 2010). The ubiquity of chromium in the environment can be traced in natural waters due to its extensive use in a variety of industries like electroplating and tanning industries, dyeing, sanitary landfill leaching, and water-cooling towers (Han et al. 2007). Until now, various sensor systems have been reported before (Margui et al. 2010; Li et al. 2011; Xin et al. 2012). To circumvent this problem low cost, sensitive sensor to be developed.

Therefore, the objectives of our present work include (i) rapid synthesis of AgNPs by using *Anacardium occidentale* plant leaves. To the best of our knowledge, there were no reports published for the rapid green synthesis of silver NPs by the use of *A. occidentale* fresh leaves extract at room temperature/higher temperature, whereas Sheny et al. (2011) were synthesized AgNPs by dried powder of *A. occidentale* (Sheny et al. 2011) (ii) developing a novel probe for sensing chromium ions [Cr(VI)] by the as prepared AgNPs, (iii) characterization of the synthesized NPs using UV–Visible spectrophotometer, theoretical particle size, XRD, SEM and TEM.

Materials and methodology

Materials

A. occidentale leaves were obtained from the plantations of Udaya School of Engineering (USE), Vellamodi and washed thoroughly with Double Distilled Water (DDW). The plant leaves without stems were cut into fine pieces and used for the experiments. Other chemicals for the experiments were procured from HiMedia and Sigma Aldrich.

Methods

Preparation of extracts

Here aqueous extracts were prepared from *A. occidentale* fresh leaves. In brief, 10 g of fresh leaves was packed down into the beaker containing 100 ml of DDW. Then, they were boiled for 30 min at three different temperatures 60, 80 and 100 °C, respectively, and thus the extract formed was filtered using Whatman Grade 1 filter paper (pore size 25 μm).The filtrate was further filtered through

0.6-μm filter and used for the further experiments. These aqueous extracts were stored for further synthesis of NPs.

Synthesis of silver nanoparticles by leaf extracts

1 mM of AgNO₃ was dissolved in 100 ml of DDW and beaker was placed on the magnetic stirrer. To that the aqueous extract was added in a dropwise manner and vigorous stirring was given. Reactions were stopped when the colloidal solution becomes brownish black.

Silver nanoparticle synthesis by gallic acid

It was expected that gallic acid acted as the premier reducing agent for the synthesis of AgNPs from *A. occidentale* leaves extract since the aqueous leaves extract of *A. occidentale* contains gallic acid. Even though the aqueous extract contains protocatechuic, *p*-hydroxybenzoic, cinnamic, *p*-coumaric and ferulic acids (Kogel and Zech 1985; Lin et al. 2010) specifically gallic acid was chosen to study the synthesis of nanoparticles. 2 % stock solution of gallic acid was prepared and used for further experiments. Synthesis protocol was the same which has been used for the aqueous extract. In brief, 1 mM AgNO₃ was dissolved in 100 ml DDW and the stirring was continued. To that, 2 % of gallic acid was added drop wise till the brownish black color was observed.

UV–Visible spectrometer characterization

Preliminary characterization of the silver nanoparticles was carried out using UV–Visible spectroscopy. The reduction of AgNO₃ to the AgNPs was monitored by measuring the UV–Visible spectra of the solutions after diluting the sample with DDW water in quartz cuvette. The spectra were recorded on Intech spectrophotometer from 300 to 600 nm. DDW was used as blank. The spectra recorded were then replotted in origin 8 software.

Theoretical size prediction

Theoretical predictions of the SPR peak (nanoparticle size) were made using Mie calculations, performed with software "MiePlot v.4.3" which is based on the Mie theory. The size of the surface of refractive index mismatch is expressed as a size parameter x:

$$x = 2\pi r n_{med}/\lambda. \tag{1}$$

By this model, we have theoretically calculated the particle size distribution of the solution by plotting the scattering efficiency as a function of wavelength. The sphere was selected as silver and the surrounding medium was selected as water. The wavelength range was selected from 300 to 600 nm. The corresponding graph obtained from this model was compared with the experimental data to derive the theoretical particle size. The size of the particles was also estimated using XRD by Debye–Scherrer equation, SEM and TEM.

Particle size distribution

Size distribution of the synthesized AgNPs and its polydispersity was checked using a particle size analyzer. The colloidal NPs were analysed by Malvern Instruments Nano. Particle size was arrived based on the measuring the time-dependent fluctuation of scattering of laser light by the nanoparticles undergoing Brownian motion.

XRD

AgNPs colloidal solution was centrifuged at 8,000 rpm for 15 min then the pellet formed were washed thrice with DDW and finally with 100 % ethanol. Then it was poured on the petriplates and allowed to dry in the hot air oven. Then the dried NPs were scrapped from petriplates and was used for further characterization and application studies. The formation and quality of compounds were checked by XRD technique. XRD was done at CECRI-CSIR Karaikudi, Tamil Nadu, India. PANalytical (X'per PRO) was used to record the diffraction pattern of the synthesized NPs. Spin-coated AgNPs on glass substrate were recorded in a wide range of Bragg angles 2θ at a scanning rate of $2° \text{ min}^{-1}$.

TEM and SEM characterization

The morphology of the synthesized NPs was determined by scanning electron microscopy (SEM) and transmission electron microscopy (TEM). For SEM analysis, thin films of the sample were prepared on a carbon-coated copper grid by simply dropping a very small amount of the sample on the grid, with excess solution being removed using blotting paper. FEI Quanta FEG 200 instrument used for the morphology analysis. For TEM studies, the solution containing the nanoparticles was diluted and a drop of it was placed on copper grid and allowed to dry in vacuum. TEM photographs were recorded using JEOL 3010.

Colorimetric detection of Cr(VI)

Colorimetric detection of Cr(VI) was carried out by adding 350 μl of Cr(VI) to 650 μl of freshly prepared AgNPs and checked for instant coloration. Absorption spectra of the final mixture were recorded using cells with 1 cm path length.

Results and discussion

There are several reports has been published for the synthesis of AgNPs by both chemical and biological reduction (Yu 2007; Tan et al. 2002; Petit et al. 1993; Vorobyova et al. 1999; Vilchis-Nestor et al. 2008; Shiv Shankar et al. 2004; Abu Bakar et al. 2007; Vigneshwaran et al. 2006; Chandran et al. 2006; Shankar et al. 2004, 2005; Philip 2009; Narayanan and Sakthivel 2011), but still we need a standard strategy for the synthesis of AgNPs with good stability and almost neutral toxicity. In this present study, we attempted to synthesize the NPs with good stability from *A. occidentale* (locally named as Kolla maram, Tamil Nadu, India) leaf extracts extracted at different temperatures 60, 80 and 100 °C, respectively.

The aqueous leaf extract of *A. occidentale* contains gallic acid, protocatechuic, *p*-hydroxybenzoic, cinnamic, *p*-coumaric and ferulic acids (Kogel and Zech 1985; Lin et al. 2010) with high potential of antioxidant and antimicrobial activities. On adding the extracts to the 1 mM $AgNO_3$ with continuous stirring, the color was changed from transparent to brownish black within 5 min. Rapid reduction was observed with all the three extracts. Although the reduction by gallic acid took more than 1 h. The appearance of brownish black color was due to the excitation of surface plasmon vibrations and it provides a convenient spectroscopic signature to indicate the formation of AgNPs (Henglein 1993). This rapid synthesis is advantageous in our present study. It is quite much more faster than the other previous plant extract-based synthesis of AgNPs (Kumara et al. 2012; Kreibig and Volmer 1995; Saha and Orvig 2010).

The mechanism of formation of NPs can be explained by the following: when the concentration of metal atoms in solution reaches supersaturation, nucleation burst takes place. In the subsequent step, the nuclei formed grow as primary particles by the diffusional capture of remaining atoms which were in excess of the solubility concentration (Kumar et al. 2012).

UV–Visible spectroscopy characterization

After obtaining the brownish black color, the as prepared AgNPs by green chemistry principle were characterized by UV–Visible spectroscopy. UV–Visible spectroscopy is one of the important techniques to discover the formation and stability of metal nanoparticles in aqueous solution. Metallic nanoparticles display a characteristic optical absorption spectra in the UV–Visible region called SPR. The physical origin of light absorption of metallic nanoparticle is the coherent oscillation of the conduction electron induced by the interacting electromagnetic field (Xia and Halas 2005). When a small spherical metallic

nanoparticle is irradiated by light, the oscillating electric field causes the oscillation of conduction electron to oscillate coherently. When electron cloud is displayed relative to the nuclei a restoring force arising coulomb attraction between electrons and nuclei that results in oscillation of electron cloud relative to the nuclear framework. These resonance is known as SPR and are actually small particle effect since they are absent in their individual atom, as well as in their bulk. Electrons conform to a specific vibration mode by particle size and shape.

Figure 1a shows the SPR position of the synthesized AgNPs by using *A. occidentale* leaf extracts extracted at different temperature namely 60, 80 and 100 °C. Absorption maxima of the synthesized AgNPs were 415 ± 0.68 nm, 400 ± 1.45 nm and 410 ± 0.98 nm at the different extraction temperature 60, 80 and 100 °C, respectively. This red or blue shift of the SPR position in between the reactions of different extract leads to different size of NPs.
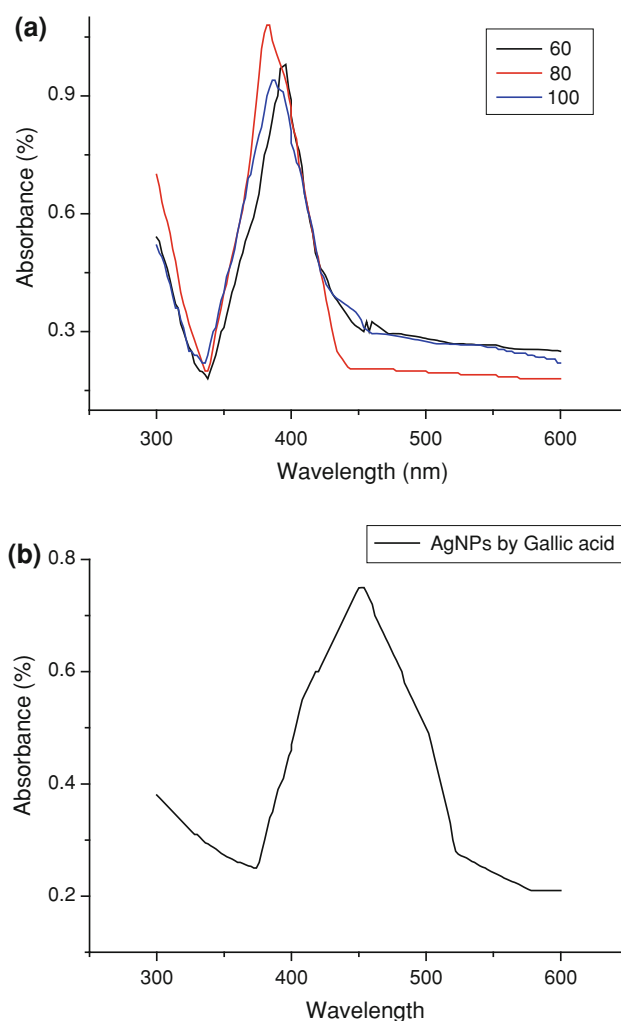
Fig. 1 **a** UV–Visible spectrum of the synthesized AgNPs at different temperature of extract from *Anacardium occidentale*. **b** UV–Visible spectrum of the synthesized AgNPs using gallic acid

Figure 1b shows the SPR position of the AgNPs synthesized by gallic acid. Maximum red shift was observed in the gallic acid reduction reaction, when comparing SPR position of gallic acid synthesized AgNPs with the AgNPs synthesized by aqueous extract. In addition, the time for the reduction reaction is also more in the case of reduction by gallic acid. The reason for the rapid reduction by aqueous extract is due to the other compounds (Kogel and Zech 1985; Lin et al. 2010) present in it.

Particle size prediction by Mie plot

Theoretical particle size of the experimental AgNPs was calculated by Mie plot v4.3 software. Particles were assumed to be sphere and might be polydisperse and a standard deviation of 10 % was used. Algorithm of Mie plot software based on the principle of Mie scattering from sphere particles. From the obtained absorption maxima of the experimental values, the theoretical particle sizes were calculated using MiePlot. We made an attempt to derive the practical relationship correlating the theoretical particle size from the absorption maxima.

Supplementary Fig. S1a shows the relationship between the standard SPR position and the assumed particle size. With the increase in particle size there was red shift in the SPR position (increase in wavelength). SPR position with the assumed particles sizes approximated with linear function. The theoretical fitted linear function was to be

$$y = 1.3209x + 343.38 \qquad (2)$$

with the R^2 value of 0.9852.

Using that empirical linear equation, theoretical particle size was calculated for the experimentally synthesized AgNPs at different temperatures. This theoretical particle size was compared with the particle size analysed by DLS was shown in Supporting Fig. S1b. PDI values of the as prepared AgNPs were tabulated in Table 1. Theoretical particle size were 53.7, 43.2, 48.6 nm and the DLS measured particle size were 59.2 ± 1.78, 42.3 ± 1.16, 53.4 ± 4.67 nm at the temperatures 60, 80, 100 °C, respectively. Mie plot calculates particle size using scattering efficiencies as a function of wavelength. In general, for smaller radius particles, light absorption is more and for larger particles light scattering becomes the dominant process (Sileikaite et al. 2009).

Table 1 Particle size and poly dispersity index of the synthesized AgNPs

Extract temperature (°C)	Particle size (nm)	PDI
60	59.2 ± 1.78	0.218 ± 0.023
80	42.3 ± 1.16	0.196 ± 0.0178
100	53.4 ± 4.67	0.268 ± 0.026

Henglein reported that when electrons are donated to the particles the surface plasmon band shifts to the blue and when holes are injected to the clusters it turns to the red. In the case of bare clusters (which can be positively or negatively charged), the Mie theory accounts for the nature of the plasmon shifts observed (Goia and Matijevic 1999). All the experiments were done in triplicates and mean values were taken for plotting the graphs.

Stability of the synthesized Ag NPs

Stability is one of the important factor for all the NPs. Our AgNPs synthesis reaction is very rapid when comparing with the other previous reported methods (Kumara et al. 2012; Kreibig and Volmer 1995; Saha and Orvig 2010) so this made us to think of checking the stability of our synthesized AgNPs. UV–Vis spectra were recorded for the AgNPs by A. occidentale leaf's different extracts against day of the incubation. Figure S2a shows the plot of SPR position of the AgNPs versus day. It revealed that A. occidentale leaf 60 C extract showed stability till 6th day of incubation at room temperature, after that SPR position was increased (red shift was observed) from 415 ± 0.69 to 492 ± 1.49 on its 20th day of the incubation whereas 100 °C extract synthesized AgNPs showed stable SPR position till its 7th day after that red shift was observed and on its 20th day of incubation SPR position was found at 460 ± 2.3 nm. However, 80 °C extract synthesized AgNPs showed highest stability till its 11th day after that red shift was attained that is from 400 ± 1.38 to 438 ± 2.61. The increase in intensity could be due to increase in amount of the absorbing species present in the aqueous solution (Li et al. 2007). After attaining the stability of SPR position against its day interval this SPR position was fitted with theoretical particle size which was calculated using Mie Plot v4.3 software. Figure S2b showing the respective particle size change during the incubation period. It revealed that 60 °C extract synthesized AgNPs size was increased from 54 ± 0.41 to 112 ± 2.65 nm and 80 °C extract synthesized AgNPs size was increased from 43 ± 0.69 to 72 ± 1.58 nm and 100 °C extract synthesized AgNPs size was increased from 48 ± 0.92 to 90 ± 2.16 nm.

Stability of the AgNPs was also checked by potentiometric measurements. This was shown in Fig. S2c. This results were comparable with the stability of the SPR position and its theoretical particle size. Apparent changes were observed in all the cases. Changes observed after 6th day in the case of AgNPs synthesized by 60 °C extract and for 100 °C it was observed from 7th day and most stable AgNPs synthesized by 80 °C were shown changes from its 11th day. From these stability experiments, we concluded that the 80 °C extract reduce the silver ions effectively with

good stability and then this 80 °C extract synthesized AgNPs were characterized by XRD, SEM and TEM.

Sensing Cr(III)

As prepared colloidal AgNPs from both the extracts were confirmed by the typical strong plasmon resonance band at 415 ± 0.68, 400 ± 1.45 and 410 ± 0.98. Cr(VI) (1 mM) were interacted with both colloidal AgNPs and intense color change was observed from brownish black to purple due to aggregation of the particles. The aggregation was commensurate with the red shift of the UV–Visible spectra. The plasmon band centered on 390 nm shifted to the right forming a distinct second peak at 510 nm with 60 °C extract, with the 80 °C extract distinct peaks were observed at 400 and 509 nm and with the 100 °C extract peak shifts were observed from 415 to 510 nm (Fig. 2a–c). This

second peak was might be formed due to the aggregation of the particles with Cr(VI). Particle size analysis was done to corroborate the results with the UV spectrophotometric finding. The average hydrodynamic diameter of the un-interacted particle was almost tenfolds lower than the interacted particles with Cr(VI) (Fig. 2d).

Selectivity and sensitivity of the AgNPs probe

The selectivity of the sensor for Cr(VI) was evaluated by monitoring the absorbance response in the presence of other heavy metal ions including Cr(III), Mg(II) (Magnesium chloride), Mn(II) (Manganese chloride), Ca(II) (Calcium chloride), Fe(II) (Ferric chloride) and Zn(II) (Zinc sulphate) at the concentration of 1 mM. The results showed an excellent selectivity of the sensor for Cr(VI) and moderate reliability for Cr(III). The results obtained clearly
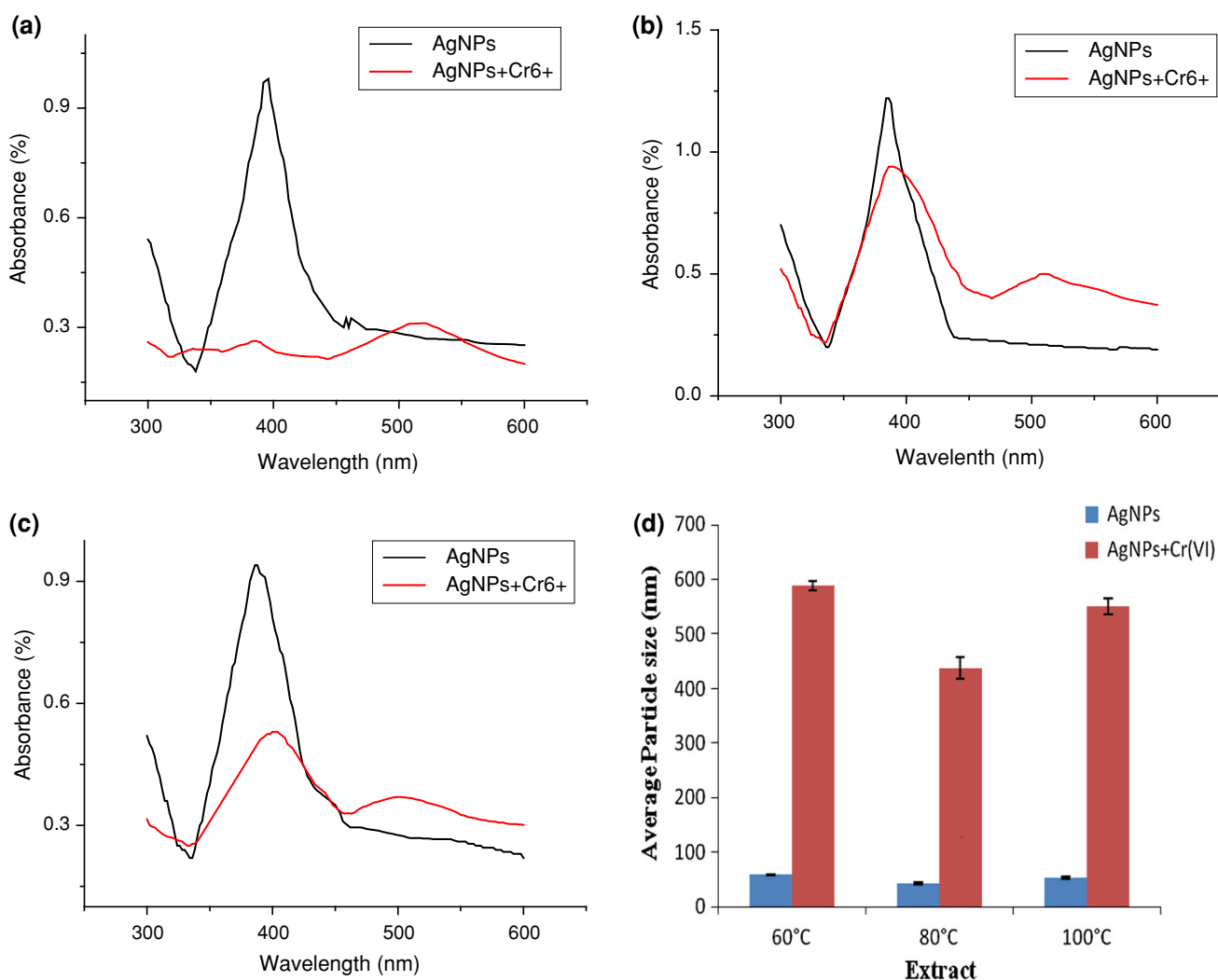
Fig. 2 **a** UV–Visible spectra of 60 °C extract synthesized AgNPs and its interaction with Cr(VI). **b** UV–Visible spectra of 80 °C extract synthesized AgNPs and its interaction with Cr(VI). **c** UV–Visible spectra of 100 °C extract synthesized AgNPs and its interaction with Cr(VI). **d** Particle size of AgNPs colloidal solution before and after interaction with the Cr(VI)

indicate that except Cr(VI) and Cr(III) no other heavy metal tested exhibited any distinct color change (Fig. 3a, b). In addition, UV–Vis graphs also showed no existence of peak at around 510 nm in the other tested heavy metals except Cr(VI) and Cr(III) (data not shown).

To confirm the sensitivity of the colloidal AgNPs with the Cr(VI), colloidal AgNPs were interacted with different concentration of Cr(VI) ranging from 10 to 100 nM. AgNPs synthesized from 60 and 100 °C were not sensitive that much since it did not show intense color change with respect to the UV spectrometric peak shift when reducing the concentration of Cr(VI) (data not shown). Hence, 80 °C extract synthesized AgNPs was alone taken for the sensitivity experiments.

Different concentration of Cr(VI) ranging from 10 mM to 100 nM were interacted with the as prepared AgNPs.

UV–visible peaks were recorded before and after interaction with Cr(VI), results are shown in Fig. 3c (Supplementary Fig. S3 shows all the concentration UV–Visible peaks). Particle size analysis clearly showing that increase in hydrodynamic particle diameter is proportional to the aggregation of AgNPs with respect to the addition of concentration of Cr(VI) which is also responsible for the color change. Table 2 shows the particle size and polydispersity index (PDI) of the colloidal AgNPs before and after interaction with different concentration of Cr(VI). It was confirmed that after interaction of Cr(VI) with the colloidal AgNPs PDI of the solution increased it clearly showed it was due to the aggregation of the particles. Figure 3d shows the corresponding color changes with the aggregation of particles. A fine degradation of color was observed from dark purple to pink as the concentration of the Cr(VI) was reduced from mM to nM.
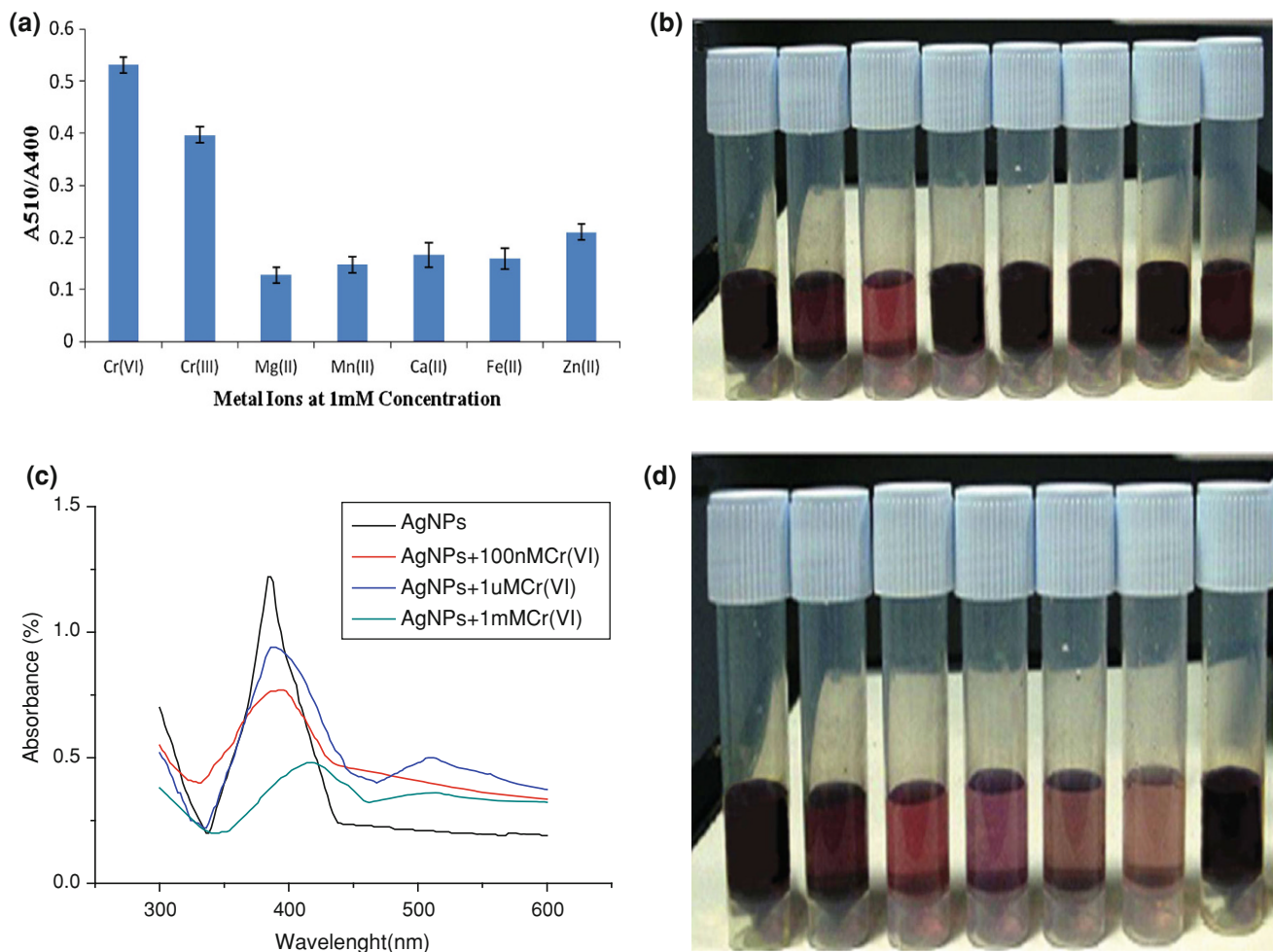
Fig. 3 **a** Absorbance ratio (A_{510}/A_{400}) comparison with different metal ions. **b** Photographic images of AgNPs colloidal solution with different metal ions [From *left* to *right*: Cr(VI), Cr(III), Mg(II), Mn(II), Ca(II), Fe(II), Zn(II)]. **c** UV–Visible Spectra of synthesized colloidal AgNPs with different concentration of Cr(VI) (AgNPs Control, 1 mM, 1 μM and 100 nM). **d** Photographic images of AgNPs colloidal solution with different concentration of Cr(VI) [From *left* to *right*: AgNPs control, AgNPs + 10 mM Cr(VI), AgNPs + 1 mM Cr(VI), AgNPs + 100 μM Cr(VI), AgNPs + 10 μM Cr(VI), AgNPs + 1 μM Cr(VI), AgNPs + 100 nM Cr(VI)]

Table 2 Particle size and polydispersity index of the colloidal AgNPs before and after interaction with Cr(VI)

Concentration of CR(VI) added	Particle size (nm)		Poly dispersity index (PDI)	
	Before addition	After addition	Before addition	After addition
10 mM	42.7 ± 0.83	487.4 ± 0.75	0.198 ± 0.018	0.486 ± 0.01
1 mM	41.64 ± 1.23	400.6 ± 2.49	0.194 ± 0.02	0.428 ± 0.028
100 μM	42.3 ± 0.89	287.9 ± 3.71	0.196 ± 0.001	0.359 ± 0.017
10 μM	42.3 ± 1.17	192.3 ± 2.18	0.196 ± 0.015	0.304 ± 0.025
1 μM	42.4 ± 0.18	97.8 ± 3.74	0.197 ± 0.04	0.263 ± 0.015
100 nM	41.9 ± 1.34	44.6 ± 2.56	0.195 ± 0.026	0.202 ± 0.018

Possible mechanism of sensing

We observed that the color of the colloidal solution AgNPs with Cr(VI) abruptly turned into purple then to pink when decreasing the concentration of Cr(VI). This is because of the reductants (protocatechuic/p-hydroxybenzoic/cinnamic/p-coumaric/ferulic acids) present in the fresh leaf aqueous extract and the added Cr(VI). This reductants reduce Cr(VI) to Cr(III) which in turn interacted with the capping agent produced from the leaf extract. This leads to form the aggregation of particles due to the ligand-receptor interaction between the Cr(VI) and the capping agent present in the solution. Possible mechanism of Cr(VI) colorimetric sensing by the as prepared AgNPs was diagrammatically represented in Fig. 4.

To prove that the color change was owing to interaction of Cr(III) with the capping agents present in AgNPs colloidal solution, the nanoparticles dispersion was interacted with Cr(III) solutions in the same range of concentrations. In this case also a linear correlation was observed up to 1 μM as in case of Cr(VI) (Fig. 5a, b). Hence, we assume that the highly selective aggregation of AgNPs on addition of Cr(VI) is mainly related to the chelation of Cr(III)

formed by reduction in Cr(VI), with capping agents present on the as synthesized AgNPs.

The synthesis of Ag NPs was achieved by *A. occidentale* based biosynthesis to yield monodispersed particles. Ag-NPs in aqueous solution are stabilized against aggregation due to the negatively charged ions present in the colloidal solution electrostatically repelling against Van der Waals attraction between AgNPs (40–60 nm). Each Cr(III) forms complexes with AgNPs colloidal solution. Thus, Cr(III) can act as cross-linking agent for pairs of capping agents in the AgNPs, thereby inducing the aggregation of AgNPs. This causes a rapid, brownish black-to-purple color change. We have made use of this property to design the sensor for Cr(VI). We have made sensitivity test also to prove our sensor system is only for the detection of Cr(VI)/Cr(III).

Characterization of AgNPs

80 °C extract of *A. occidentale* was shown good stability and better detection efficiency among three extracts we used. So, 80 °C extract was used for characterization studies.

**Fig. 4** Possible mechanism of Cr(III) sensing by the AgNPs probe

● Cr(VI)
● Cr(III)
● AgNPs
◗ Capping agent from *Anacardiuun Occidentale* leaf extract
● Agglomerated AgNPs
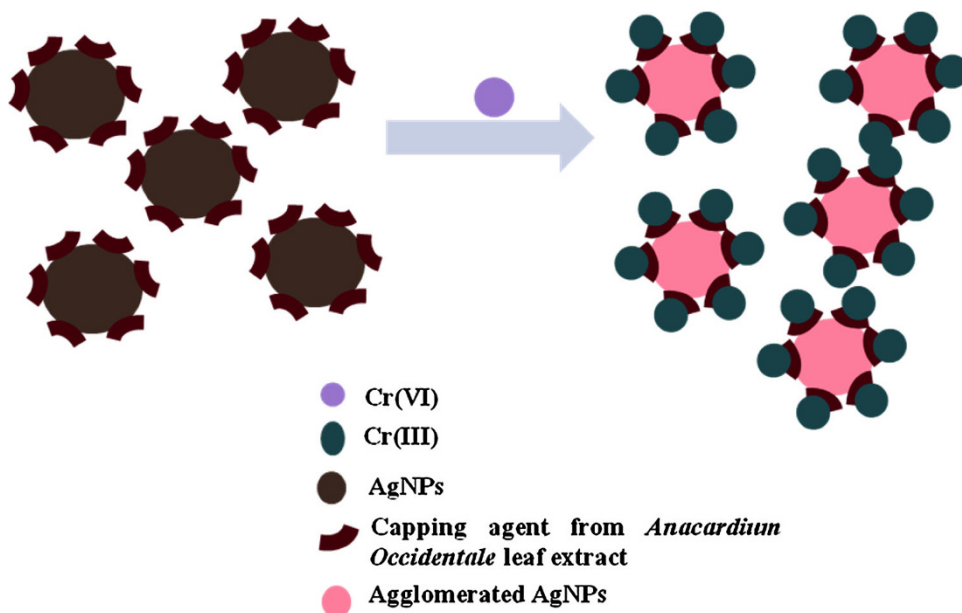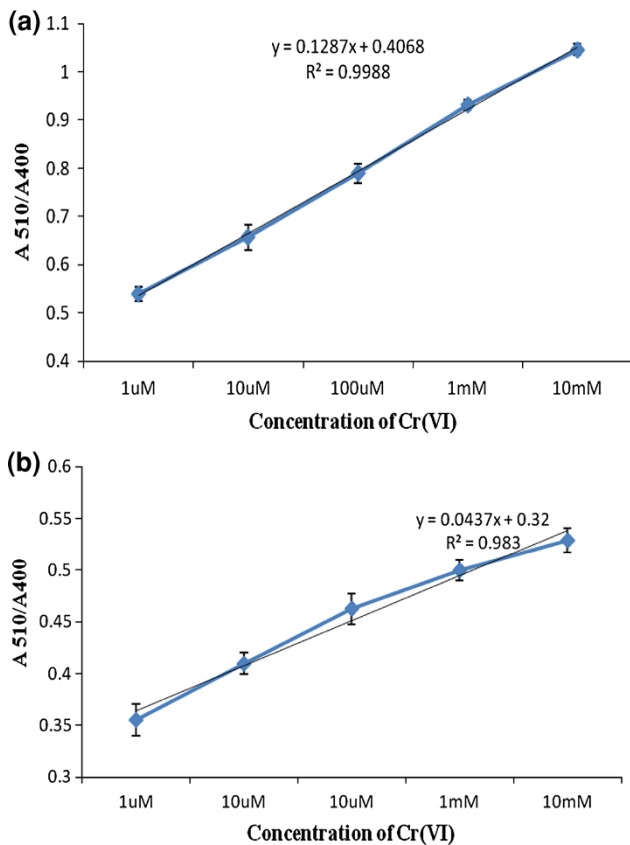
Fig. 5 **a** Absorbance ratio (A_{510}/A_{400}) against different concentration of Cr(VI). **b** Absorbance ratio (A_{510}/A_{400}) against different concentration of Cr(III)

The X-ray diffraction (XRD) is one of the valuable research tools to determine the crystal structure of the NPs and to calculate the crystalline particle size. Purified AgNPs was evaluated by powder XRD for identifying its crystal behavior. Powder XRD pattern of the synthesized AgNPs showed four distinct diffraction peaks at 37.95, 45.95, 64.22 and 76.74 which could be assigned to (1 1 1), (2 0 0), (2 2 0) and (3 1 1) of face centered cubic (fcc) of AgNPs (Gopinath et al. 2012) (Fig. 6a). There were no diffraction peaks for corresponding to the precursor (AgNO$_3$) and/or by-products (such as silver oxide) were observed, which confirms that only metallic Ag was formed in situ by *A. occidentale* extract reaction. The intensity of peaks reflects the high degree of crystallinity of the synthesized AgNPs. However, the diffraction peaks are broad which indicates that small crystallite size is obtained. This is in good agreement with the report done by Sheny et al. (2011) and Kumar et al. (2012).

The lattice constant was in agreement with the database of Joint Committee on Powder Diffraction Standards (JCPDS. No. 01-087-0597). Average grain size was measured by well known Scherrer formula, $D = \kappa\lambda/\beta\cos\theta$ where κ is Sherrer constant which equals to 1, λ is
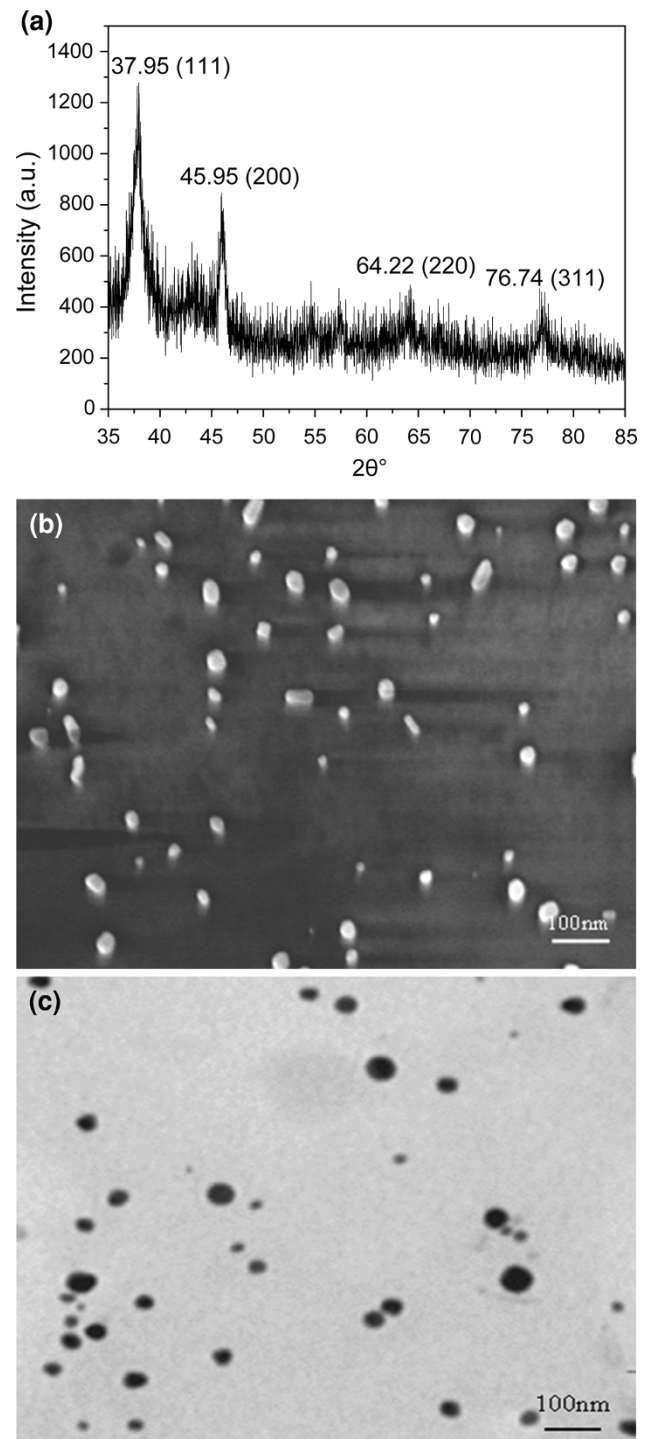
Fig. 6 **a** XRD characterization of the synthesized AgNPs. **b** SEM characterization of the synthesized AgNPs. **c** TEM characterization of the synthesized AgNPs

wavelength of the X-ray passed (0.1541 nm), β is full width at half maximum (FWHM), θ is the diffraction angle corresponds to the lattice plane. Average grain size was calculated by Scherrer formula as 48.6 nm.

مدينة الملك عبدالعزيز
KACST للعلوم والتقنية
Springer

Figure 6b shows representative SEM image which were recorded at different magnifications from drop-coated films of the AgNPs synthesized by treating AgNO$_3$ solution with *A. occidentale* leaf extract. The resulting AgNPs were predominantly sphere and of almost uniform in size. Higher magnification showed the average diameter of these sphere nanoparticles to be about 40–60 nm. TEM measurements were conducted in order to estimate the exact particle size and size distribution for the as prepared AgNPs. Figure 6c shows representative TEM image of the as prepared AgNPs. This fig revealed that individual silver particles with spherical shapes without any aggregates. Therefore, our assumption was correct for the theoretical prediction particle size since it was assumed to be spherical. The separation between the AgNPs seen in the TEM and SEM image could be due to capping effect of *A. occidentale* extract. This may explain the UV–Visible spectroscopy measurements, which is characteristic of well-dispersed AgNPs. It was noticed that the size ranges from 50 to 60 nm. This size supporting our SEM characterization.

Application study

To confirm the practical application capability of AgNPs probe prepared by *A. occidentale* extract, the concentration of Cr(VI) in real water samples (tap water of Udaya School of Engineering and a pond near by Manavalakkurichi, Nagercoil) was determined by applying this assay method. Absorbance ratios of tap water and the pond water were noted to be 0.5 ± 0.046 and 0.607 ± 0.109. By comparing with the calibration curve, Fig. 5a the concentration of Cr(VI) present in the real sample was measured as 0.2–1 μM (5–50 μg/L) in the case of tap water and pond water it was 3–5 μM (150–250 μg/L) based on the detection results which is an good agreement detection result of 14 ± 3 μg/L (within the range of 5–50 μg/L) for tap water and 198 ± 6 μg/L (within the range of 150–250 μg/L) for the pond water by ICP-AES method. Our results corroborate range of Cr(VI) concentrations in the natural water matrices with the previous research report (Handa 1988). Thus, our results demonstrated that the currently designed colorimetric method is applicable for the detection of Cr(VI) in real environmental water samples.

Conflict of result

The authors declare that they do not have conflict of interest.

Conclusion

In this present study, we have demonstrated the use of fresh leaves extract as the reducing and capping agent for the rapid synthesis of spherical shaped AgNPs at room temperature followed by green chemistry principle. From the absorption maxima obtained by UV–Visible spectrometry studies, the theoretical particle size was determined using MiePlot v4.3 software and an empirical relationship was derived correlating the absorption maxima and the particle size. 80 °C extract synthesized AgNPs were more stable. The synthesized AgNPs were involved for the detection of Cr(VI). Both the extracts were involved in this study, 80 °C extract synthesized AgNPs showed intense shift in UV–Visible spectrum. Detection limit of the as prepared AgNPs probe was measured as 1 μM. Mechanism behind this sensing process is Cr(VI) was reduced to Cr(III) by the compounds present in the colloidal AgNPs solution and this Cr(III) binds with the capping agent present in the solution and leads to aggregation of AgNPs and color change occurred. Tap water of Udaya college of Engineering and pond water nearby Manavalakkurichi, Kanyakumari District, Tamil Nadu were collected and analysed for the level of Cr(VI) present in it. It was measured as 0.2–1 μM (5–50 μg/L) for the tap water and 3–5 μM (150–250 μg/L) for the pond water which was compared with the common detection instrument ICP-AES and found out as 14 ± 3 μg/L (within the range of 5–50 μg/L) for tap water and 198 ± 6 μg/L. Finally, the efficient 80 °C extract synthesized AgNPs was further characterized by XRD, SEM and TEM. All the size characterization studies revealed that the particle size were around 40–60 nm. After characterizing our AgNPs. This studies formed the base and prompted us for the development of lateral flow strip assay for Cr(VI) detection. Our future research will describe in detail strip development.

References

Abu Bakar NHH, Ismail J, Abu Bakar M (2007) Synthesis and characterization of silver nanoparticles in natural rubber. Mater Chem Phys 104:276–283

Alivisatos AP (1996) Semiconductor clusters, nanocrystals, and quantum dots. Science 271:933–937

Bae CH, Nam SH, Park SM (2002) Formation of silver nanoparticles by laser ablation of a silver target in NaCl solution. Appl Surf Sci 197:628–634

Basu A, Saha R, Mandal J, Ghosh S, Saha B (2010) Removal of hexavalent chromium by an aromatic alcohol. J Biomed Sci Eng 3:735–741

Broadhurst CL, Domenico P (2006) Clinical studies on chromium picolinate supplementation in diabetes mellitus—a review. Diabetes Technol Ther 8:677–687

Bruchez M, Moronne M, Gin P, Weiss S, Alivisatos AP (1998) Semiconductor nanocrystals as fluorescent biological labels. Science 281:2013–2016

Chandran SP, Chaudhary M, Pasricha R, Ahmad A, Sastry M (2006) Synthesis of gold nanotriangles and silver nanoparticles using aloevera plant extract. Biotechnol Prog 22:577–583

Coe S, Woo WK, Bawendi M, Bulovic V (2002) Electroluminescence from single monolayer of nanocrystals in molecular organic devices. Nature 420:800–803

Gardea-Torresdey JL, Parsons JG, Dokken K, Peralta-Videa J, Troiani HE, Santiago P, Jose-Yacaman M (2002) Formation and growth of Au nanoparticles inside live Alfalfa plants. Nano Lett 2:397–401

Gardea-Torresdey JL, Gomez E, Peralta-Videa J, Parsons JG, Troiani HE, Jose-Yacaman M (2003) Alfalfa sprouts: a natural source for the synthesis of silver nanoparticles. Langmuir 19:1357–1361

Goia DV, Matijevic E (1999) Tailoring the particle size of monodispersed colloidal gold. Colloids Surf A: Physicochem Eng Asp 146:139–152

Gopinath V, MubarakAli D, Priyadarshini S, Meera Priyadharsshini N, Thajuddin N, Velusamy P (2012) Biosynthesis of silver nanoparticles from *Tribulus terrestris* and its antimicrobial activity: a novel biological approach. Colloids Surf B 96:69–74

Han ZQ, Qi L, Shen GY, Liu W, Chen Y (2007) Determination of chromium(VI) by surface plasmon field-enhanced resonance light scattering. Anal Chem 79:5862–5868

Handa BK (1988) Occurrence and distribution of chromium in natural waters of India. Adv Environ Sci Technol 20:189–214

Henglein A (1993) Physicochemical properties of small metal particles in solution: "microelectrode" reactions, chemisorption, composite metal particles, and the atom-to-metal transition. J Phys Chem 97:5457–5471

Husseiny MI, Abd El-Aziz M, Badr Y, Mahmoud MA (2007) Biosynthesis of gold nanoparticles using *Pseudomonas aeruginosa*. Spectrochim Acta A 67:1003–1006

Kaviya S, Santhanalakshmi J, Viswanathan B, Muthumary J, Srinivasan K (2011) Biosynthesis of silver nanoparticles using *Citrus sinensis* peel extract and its antibacterial activity. Spectrochim Acta Part A 79:594–598

Keki S, Torok J, Deak G (2000) Silver nanoparticles by PAMAM-assisted photochemical reduction of Ag$^+$. J Colloid Interface Sci 229:550–553

Kogel I, Zech W (1985) The phenolic acid content of cashew leaves (*Anacardium occidentale* L.) and of the associated humus layer, Senegal. Geoderma 35:119–125

Kreibig U, Volmer M (1995) Optical properties of metal clusters. Springer, Berlin

Kumar R, Roopan SM, Prabhakarn A, Khanna VG, Chakroborty S (2012) Agricultural waste *Annona squamosa* peel extract: biosynthesis of silver nanoparticles. Spectrochim Acta Part A 90:173–176

Kumara K, Sinha M, Mandala B, Ghosh A, Siva Kumar K, Sreedhara Reddy P (2012) Green synthesis of silver nanoparticles using *Terminalia chebula* extract at room temperature and their antimicrobial studies. Spectrochim Acta Part A 91:228–233

Li S, Shen Y, Xie A, Yu X, Qui L, Zhang L, Zhang Q (2007) Green synthesis of silver nanoparticles using *Capsicum annum* L. extract. Green Chem 9:852–858

Li F, Liu J, Wang X, Lin L, Cai W, Lin X, Zeng Y, Li Z, Lin S (2011) Non-aggregation based label free colorimetric sensor for the detection of Cr(VI) based on selective etching of gold nanorods. Sens Actuator B—Chem 155:817–822

Lin L, Wang W, Huang J, Li Q, Sun D, Yang X, Wang H, He N, Wang Y (2010) Nature factory of silver nanowires: plant-mediated synthesis using broth of *Cassia fistula* leaf. Chem Eng J 162:852–858

Liu YC, Lin LH (2004) New pathway for the synthesis of ultrafine silver nanoparticles from bulk silver substrates in aqueous solutions by sonoelectrochemical methods. Electrochem Commun 6:1163–1168

Lukman AI, Gong B, Marjo CE, Roessner U, Harris AT (2011) Facile synthesis, stabilization, and anti-bacterial performance of discrete Ag nanoparticles using *Medicago sativa* seed exudates. J Colloid Interface Sci 353:433–444

Mallick K, Witcombb MJ, Scurrella MS (2005) Self-assembly of silver nanoparticles in a polymer solvent: formation of a nanochain through nanoscale soldering. Mater Chem Phys 90:221–224

Margui E, Fontas C, Toribio M, Guillem M, Hidalgo M, Queralt I (2010) Determination of water-soluble hexavalent chromium in clinker samples by wavelength-dispersive X-ray fluorescence spectrometry after concentration in activated layers. Appl Spectrosc 64:547–551

Naik RR, Stringer SJ, Agarwal G, Jones S, Stone MO (2002) Biomimetic synthesis and patterning of silver nanoparticles. Nat Mater 1:169–172

Narayanan KB, Sakthivel N (2011) Extracellular synthesis of silver nanoparticles using the leaf extract of Coleus amboinicus Lour. Mater Res Bull 46:1708–1713

Petit C, Lixon P, Pileni MP (1993) In situ synthesis of silver nanocluster in AOT reverse micelles. J Phys Chem 97:12974–12983

Philip D (2009) Biosynthesis of Au, Ag and Au–Ag nanoparticles using edible mushroom extract. Spectrochim Acta Part A 73:374–381

Saha B, Orvig C (2010) Biosorbents for hexavalent chromium elimination from industrial and municipal effluents. Coord Chem Rev 254:2959–2972

Sandmann G, Dietz H, Plieth W (2000) Preparation of silver nanoparticles on ITO surfaces by a double-pulse method. J Electroanal Chem 491:78–86

Sarkar M, Banthia S, Samanta A (2006) A highly selective 'off–on' fluorescence chemosensor for Cr(III). Tetrahedron Lett 47:7575–7578

Sastry M, Ahmad A, Khan MI, Kumar R (2003) Biosynthesis of metal nanoparticles using fungi and actinomycete. Curr Sci 85:162–170

Sathishkumar M, Sneha K, Kwak IS, Mao J, Tripathy SJ, Yun YS (2009) Phyto-crystallization of palladium through reduction process using *Cinnamom zeylanicum* bark extract. J Hazard Mater 171:400–404

Shankar SS, Rai A, Ankamwar B, Singh A, Ahmad A, Sastry M (2004) Biological synthesis of triangular gold nanoprisms. Nat Mater 3:482–488

Shankar SS, Rai A, Ahmad A, Sastry M (2005) Controlling the optical properties of lemongrass extract synthesized gold nano-triangles and potential application in infrared-absorbing optical coatings. Chem Mater 17:566–572

Sharma NC, Sahi S, Sudipnath J, Parsons JG, Tarasankarpal T (2007) Synthesis of plant-mediated gold nanoparticles and catalytic role of biomatrix-embedded nanomaterials. Environ Sci Technol 47:5137–5142

Sheny DS, Mathew J, Philip D (2011) Phytosynthesis of Au, Ag and Au–Ag bimetallic nanoparticles using aqueous extract and dried leaf of *Anacardium occidentale*. Spectrochim Acta A 79:254–262

Shiv Shankar S, Rai A, Ahmad A, Sastry M (2004) Rapid synthesis of Au, Ag, and bimetallic Au core–Ag shell nanoparticles using Neem (*Azadirachta indica*) leaf broth. J Colloid Interface Sci 275:496–502

Sileikaite A, Puiso J, Prosycevas I, Tamulevicius S (2009) Investigation of silver nanoparticles formation kinetics during reduction of silver nitrate with sodium. Mater Sci 15:21–27

Smetana AB, Klabunde KJ, Sorensen CM (2005) Synthesis of spherical silver nanoparticles by digestive ripening, stabilization with various agents, and their 3-D and 2-D super lattice formation. J Colloid Interface Sci 284:521–526

Swami A, Selvakannan PR, Pasricha R, Sastry M (2004) One-step synthesis of ordered two-dimensional assemblies of silver nanoparticles by the spontaneous reduction of silver ions by pentadecylphenol Langmuir monolayers. J Phys Chem B 108:19269–19275

Tan Y, Wang Y, Jiang L, Zhu DJ (2002) Thiosalicylic acid-functionalized silver nanoparticles synthesized in one-phase system. Colloid Interface Sci 249:336–345

Vigneshwaran N, Nachane RP, Balasubramanya RH, Varadarajan PV (2006) A novel one-pot 'green' synthesis of stable silver nanoparticles using soluble starch. Carbohydr Res 341:2012–2018

Vilchis-Nestor AR, Sanchez-Mendieta V, Camacho-Lopez MA, Gomez-Espinosa RM, Camacho-Lopez MA, Arenas-Alatorre JA (2008) Solventless synthesis and optical properties of Au and Ag nanoparticles using *Camellia sinensis* extract. Mater Lett 62:3103–3105

Vorobyova SA, Lesnikovich AI, Sobal NS (1999) Preparation of silver nanoparticles by interphase reduction. Colloids Surf A 152:375–379

Wang L, Wang L, Xia T, Dong L, Chen H, Li L (2004) Selective fluorescence determination of chromium(VI) with poly-4-vinylaniline nanoparticles. Spectrochim Acta Part A 60:2465–2468

Wu T, Liu C, Tan KJ, Hu PP, Huang CZ (2010) Highly selective light scattering imaging of chromium (III) in living cells with silver nanoparticles. Anal Bioanal Chem 397:1273–1279

Xia Y, Halas NJ (2005) Shape-controlled synthesis and surface plasmonic properties of metallic nanostructures. MRS Bull 30:338–348

Xin J, Zhang F, Gao Y, Feng Y, Chen S, Wu A (2012) A rapid colorimetric detection method of trace Cr(VI) based on the redox etching of Agcore–Aushell nanoparticles at room temperature. Talenta 101:122–127

Yu DG (2007) Formation of colloidal silver nanoparticles stabilized by Na$^+$–poly(γ-glutamic acid)–silver nitrate complex via chemical reduction process. Colloids Surf B 59:171–178

Zhang L, Shen YH, Xie AJ, Li SK, Jin BK, Zhang QF (2006) One-step synthesis of monodisperse silver nanoparticles beneath vitamin E Langmuir monolayers. J Phys Chem B 110:6615–6620

Zhang L, Xu C, Li B (2009) Simple and sensitive detection method for chromium(VI) in water using glutathione—capped CdTe quantum dots as fluorescent probe. Mikrochim Acta 166:61–68